

Research paper

Thermalized solution of the Galerkin-truncated Burgers equation: From the birth of local structures to thermalization

Peihua Feng^a, Jiazhong Zhang^{a,*}, Shengli Cao^a, S.V. Prants^b, Yan Liu^c^aSchool of Energy and Power Engineering, Xi'an Jiaotong University, Xi'an 710049, China^bPacific Oceanological Institute of the Russian Academy of Sciences, Vladivostok 690041, Russia^cSchool of Mechanical Engineering, Northwestern Polytechnical University, Xi'an 710042, China

ARTICLE INFO

Article history:

Received 11 March 2016

Revised 7 August 2016

Accepted 5 September 2016

Available online 13 September 2016

Keywords:

Thermalization

Truncation

Inviscid Burgers equation

ABSTRACT

Discrepancy between truncated and exact solutions of the inviscid Burgers equation is studied by the pseudo-spectral method with setting all the Fourier modes with the wavenumbers beyond a truncated wavenumber K_G to be zero. A localized short-wavelength oscillation, called as a “tyger”, appears at occurrence of the shock in the truncated solution. The “tyger” shows very different shapes depending on the way of truncation of the nonlinear term. Moreover, the birth of the “tyger” is related to a period-doubling bifurcation which is illustrated by a map constructed by an iterative method at the center of the “tyger”. In order to study the process of stability loss of the truncated wave solution, a perturbed wave is derived. The truncated wave solution loses its stability in every oscillator mode of the perturbed wave. Finally, the long-term process of thermalization is displayed by the perturbed wave coupled with a frozen wave profile containing a symmetric pair of shocks. Thermalization appears from the both sides of small structures around the center without symmetry breaking. The phenomenon of the birth of “a tyger” and its following thermalization can be understood from the view of stability loss of the truncated wave solution.

© 2016 Elsevier B.V. All rights reserved.

1. Introduction

Although turbulence is ubiquitous and has been studied for over one century since the Reynolds experiments, its nature is still not fully understood [1]. So far, the Kolmogorov theory, also called as K41, is the most successful and classical phenomenological framework to describe fully developed turbulence [2]. The most significant idea contained in K41 is the conception of energy cascade which reveals development of kinetic energy. Namely, kinetic energy is transferred from a large scale L (known as the integral length scale) to smaller and smaller scales, and the transference stops at the scale η_d at which the kinetic energy turns to heat by molecular viscosity. As to statistical properties at $Re \rightarrow \infty$, they are determined only by the scale r in the inertial range ($\eta_d \ll r \ll L$) and the energy dissipation rate per unit volume ϵ which converges to a finite and positive value rather than zero. For fully developed homogeneous isotropic turbulence, the energy spectrum $E(k)$ over the Fourier modes is described by the relation $E(k) \sim k^{-5/3}$ via the dimensional analysis in K41.

However, Hopf [3] and Lee [4] have considered turbulent flows from a very different perspective. They start from an ideal flow described by the incompressible Euler equation. Specifically, Lee applies the Galerkin truncation to a Hamiltonian system (the 3D Euler equation) and reduces the equation to a finite-dimension system in the Fourier space. The results show

* Corresponding author. Fax: +86 029 82668723.

E-mail addresses: f-peihua@stu.xjtu.edu.cn (P. Feng), jzzhang@mail.xjtu.edu.cn (J. Zhang), csl1993@stu.xjtu.edu.cn (S. Cao), prants@poi.dvo.ru (S.V. Prants), Luyan@nwpu.edu.cn (Y. Liu).

that long-term behavior of the system can be described by an equipartition of energy. In other words, the thermalized state is discovered which means that the kinetic energy distributes as $E(k) \sim k^2$ in the Fourier modes. Their studies allow to understand turbulence flows from the point of view of equilibrium statistical mechanics. Furthermore, one can link dissipative hydrodynamical description at a macroscopic level with irreversible energy loss and a conservative Hamiltonian formulation at a microscopic level using the Gibbs ensembles.

There is still, however, a contradiction that the kinetic energy distribution, $E(k) \sim k^2$, is very far from the Kolmogorov's prediction. Kraichnan and Nagarajan [5] considers the Galerkin-truncated equilibria of the 2D Euler equation otherwise. He studies the direction of energy cascade in 2D turbulence and proposes a conjecture of an inverse cascade. It even has been found that the truncated Euler system can imitate real flows governed by the Navier-Stokes equation [6]. In this sense, the process of kinetic energy transference from large scales to small ones is analogous to that of the kinetic energy transference from low wave numbers to high ones in the Fourier space. More specifically, "the high-wavenumber degrees of freedom act like a thermal sink into which the energy of low-wave-number modes excited above equilibrium is dissipated. In the limit where the sink wavenumbers are very large compared with the anomalously excited wavenumbers, this dynamical damping acts precisely like a molecular viscosity" [6].

In order to prove the statements above, Cichowlas et al. [7] simulate the 3D Galerkin-truncated Euler equation. Their results show that after a long-term transient process only high-wavenumber modes are thermalized and act as a kind of an artificial molecular reservoir leading to the effect of dissipation of low-wavenumber modes. Thus, large scale dynamics obeys (at least, approximately) to the Kolmogorov scaling which is found to be similar to that of the high-Reynolds number Navier-Stokes equations. Such phenomenon has been discovered also in other systems [8,9]. In particular, the thermalization also occurs in hydrodynamical equations with a dissipative term in the form of the Laplacian with a high power α [8].

Even more specifically, in order to display the process of thermalization, Ray simulates the simple Galerkin-truncated Burgers equation with the initial condition in the form of a single harmonic Fourier mode [10]. Curiously, after a certain time t_* as shock forms, spurious oscillations are observed in the physical space. The oscillations or a highly-organized structure occur due to a particle-wave resonance, and its symmetry breaking is considered as the onset of thermalization. It was named by Ray as a "tyger" following to the William Blake's poem "The tyger". Venkataraman [11] estimates precisely the time at which thermalization is triggered. Following the idea from Frisch et al. [12], Ray [13] connects the equilibrium statistical mechanics and out-of-equilibrium dissipative turbulence by fractal dimensions in order to study the relationship between turbulence described in K41 theory and thermalized solution.

In this study, formation of the "tygers" is explained by stability loss of the wave when pre-shock or pre-shock waves appear. In other words, a perturbed wave is amplified rather than suppressed in all directions by the shock wave. Then in order to observe the transient process from the "tygers" to a final thermalization, the localized structures are separated by the perturbed wave from the original shock wave. Discrepancy between the "tygers" obtained by two different ways of truncation is discussed in Section 2. The birth of "tygers" is related to a map constructed by the iterative method (Section 3). In Section 4, stability of the original wave before occurrence of the "tygers" is analyzed via the complex oscillator system. Moreover, the transient thermalization is displayed by the perturbed wave under a frozen wave pattern with a pair of shocks in Section 5. Conclusions are given in Section 6.

2. "Tygers" in the Galerkin-truncated Burgers equation

The spectral method is the most precise numerical method in fluid dynamics [14]. In this method, truncated errors can be damped by viscous dissipation, but it cannot be neglected if the Reynolds number is large, especially at the moment when a shock wave occurs in this study. The truncated error is represented as an aliasing error [15] which leads to "tygers". The solution, restricted to 2π periodic boundary conditions, is expanded in the Fourier modes

$$u(x, t) = \sum_{k=-\infty}^{+\infty} A_k(t) \exp(ikx). \quad (1)$$

The Galerkin-truncated solution is defined by the Galerkin projector, P_{K_G} . It plays the key role of a low-pass filter setting to zero all the Fourier components with the wavenumbers satisfying $|k| > K_G$,

$$P_{K_G} u(x, t) = \sum_{|k| \leq K_G} A_k(t) \exp(ikx). \quad (2)$$

The inviscid Burgers equation (Eq. (3)) and its truncated version (Eq. (4)), obtained by applying the projector P_{K_G} to the nonlinear term and the initial conditions, are displayed as follows:

$$\frac{\partial u}{\partial t} + u \frac{\partial u}{\partial x} = 0, \quad u(x, 0) = u_0(x), \quad (3)$$

$$\frac{\partial v}{\partial t} + P_{K_G} \left(v \frac{\partial v}{\partial x} \right) = 0, \quad v(x, 0) = P_{K_G} u_0(x). \quad (4)$$

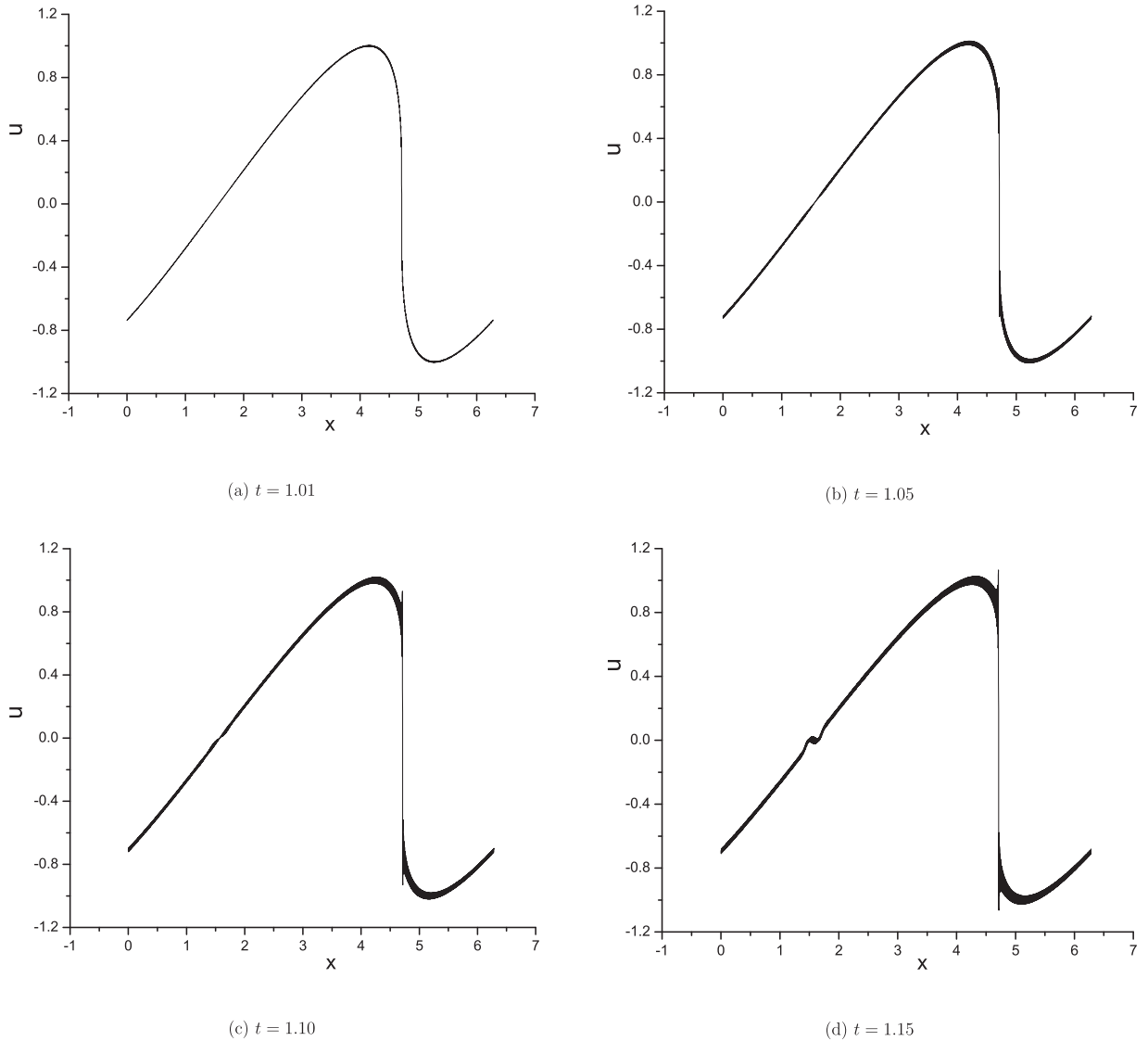


Fig. 1. The wave profiles for Eq. (4) at different time instants.

Besides Eq. (4), there also exists another way of applying the projection to the nonlinear term

$$\frac{\partial \nu}{\partial t} + (\mathbf{P}_{K_G} \nu) \left(\mathbf{P}_{K_G} \frac{\partial \nu}{\partial x} \right) = 0, \quad \nu(x, 0) = \mathbf{P}_{K_G} u_0(x). \quad (5)$$

Actually, the problem of finite-time singularities is also exists in the inviscid Burgers equation. More specifically, the solution blows up beyond a finite critical time t_* with a continuous initial wave profile. At this very moment, a cubic-root singularity of the solution, also called as a pre-shock [16], occurs because the gradient $\partial u / \partial x$ tends to infinity at the singularity point. For example, if the initial condition

$$u_0(x) = \sin(x) \quad (6)$$

is chosen, the critical time is $t_* = 1.0$. Simulation could continue beyond t_* , but it does not satisfy to the inviscid Burgers equation in a strong sense. It is because the “tygers”, explained by the wave-particle resonance mechanism [10], appear to be accompanied by the shock waves in the form of discontinuity.

In this section, it is found that the “tygers” in Eq. (4) are different from those that are obtained in Eq. (5) with the initial condition $u_0(x) = \sin(x - \pi/2)$ to show the results more clearly. The wave profiles with their details beyond the critical time are shown in Fig. 1. Number of collocation points N and the Galerkin-truncation wavenumber K_G in this simulation are chosen to be $N = 2^{14}$ and $K_G = 700$.

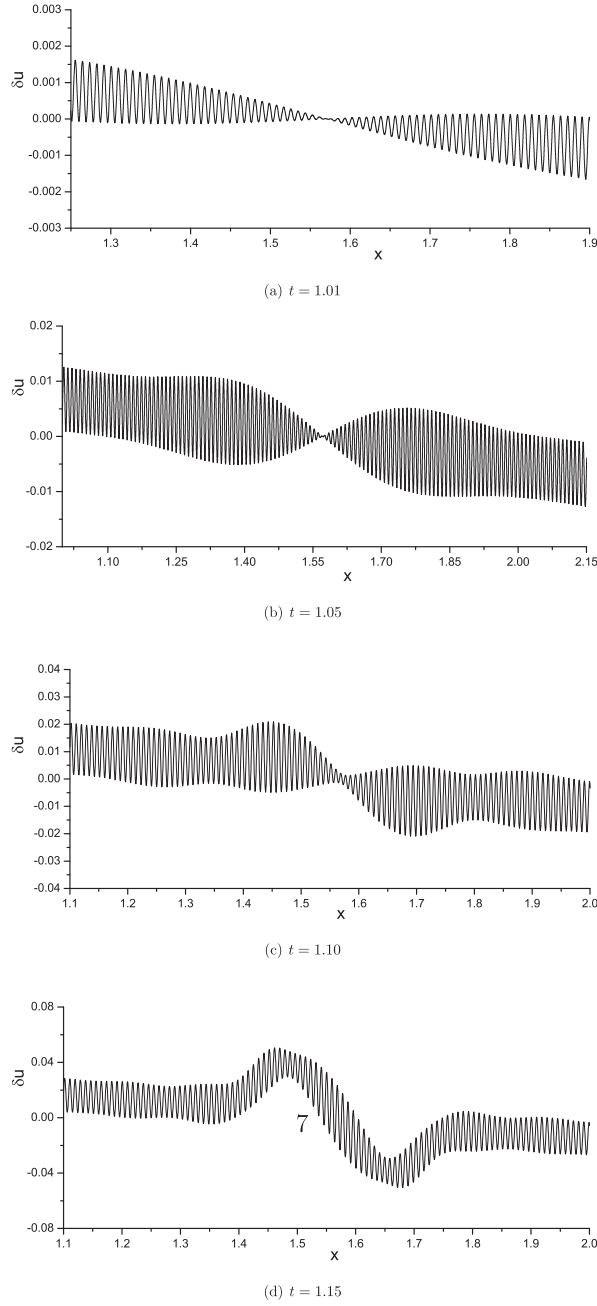


Fig. 2. “The tygers” for Eq. (4) at different time instants.

The pre-shock (a cubic-root singularity) for Eq. (4) becomes a shock wave quickly beyond the critical time as shown in Fig. 1. The bulge around the shock wave forms during almost the same time, but it grows slowly. Fig. 2 demonstrates a discrepancy between the truncated wave profile u and the untruncated wave solution U , namely,

$$\delta u = u - U. \quad (7)$$

On the contrary, the “tyger” around $x \approx 1.57$ does not occur as expected. It even seems to be suppressed slightly beyond $t_* = 1.0$. Then it begins to hunch after an obvious distortion when $t > 1.10$, approximately. After the distortion, the “tyger” grows quickly. It loses its stability and becomes a state of thermalization after a long-term transient process which is discussed in Section 5.

However, the formation of the “tygers” through Eq. (5) exhibits very different features. The wave profiles beyond $t_* = 1.0$ are shown in Fig. 3. First, the bulge grows much faster than that of Eq. (4). Second, the “tyger” around $x \approx 1.57$ occurs

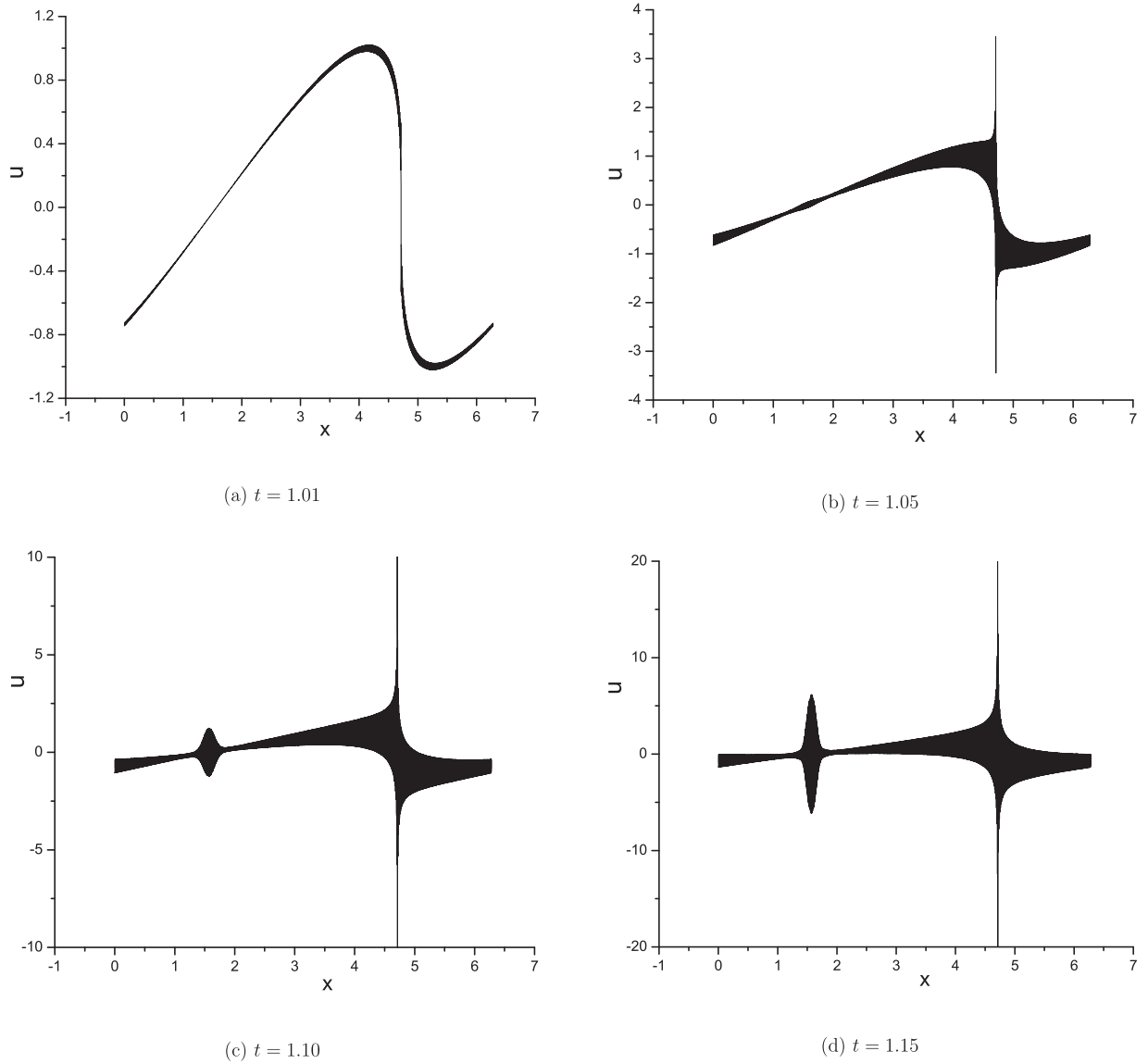


Fig. 3. The wave profiles for Eq. (5) at different time instants.

immediately when the time reaches up the critical time. Obviously, the bugle around the shock wave grows faster and invades the entire domain more quickly than the “tyger”. It is the contrary case as compared to the results in [10]. Applying the projection P_{K_G} to the velocity v and its derivative $\partial v/\partial x$ of nonlinear term in Eq. (5) means that the dealiasing technology is achieved by the projection P_{K_G} . The difference between the “tygers” shapes of Eqs. (4) and (5) caused by aliasing error suggests that the generation of “tygers” involves all Fourier modes, which agrees to the conclusion in Ref. [17]. Additionally, the frequency of solution around the center of the “tyger” seems to double shifting the hunch of the “tyger” from its center. The discrepancy δu between the wave profile and the solution at the critical time is also shown in Fig. 4.

3. Period-doubling bifurcation of the center of the “tyger”

The previous results suggest a period-doubling bifurcation at formation of the “tyger”. Zhang et al. [18] actually constructed a map from the analytical solution of the inviscid Burgers equation Eq. (3) and proved that the period-doubling bifurcation occurs at the center of “a tyger” as a pre-shock form. The analytical solution with the initial condition for Eq. (6) is

$$u(x, t) = \sin(x - ut). \quad (8)$$

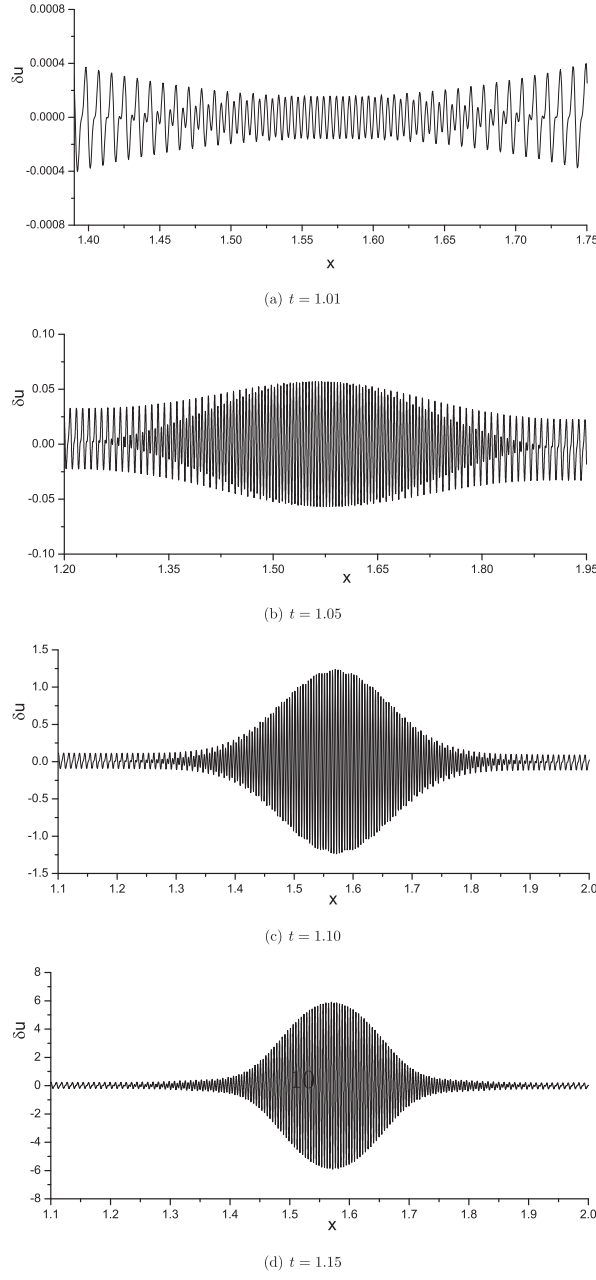


Fig. 4. “The tygers” for Eq. (5) at different time instants.

The map g is obtained by the iterative method from Eq. (8) as

$$g : u_{n+1} = \sin(x - u_n t). \quad (9)$$

As the indicator of a bifurcation, the Floquet multiplier of the map (9) at a fixed point is

$$Dg|_{u^*} = -\cos(x - u_* t). \quad (10)$$

As time goes to the critical time $t_* = 1.0$, the Floquet multiplier $Dg|_{u_*}$ approaches to -1 , which implies that a period-doubling bifurcation can occur during a finite time at $x = 0.0$.

In order to specify the process, let us consider a disturbance δu of the wave profile at the critical time t_* to be induced by a time disturbance δt . The wave profile at t_* and its disturbance are the following:

$$u = \sin(x - ut_*), \quad (11)$$

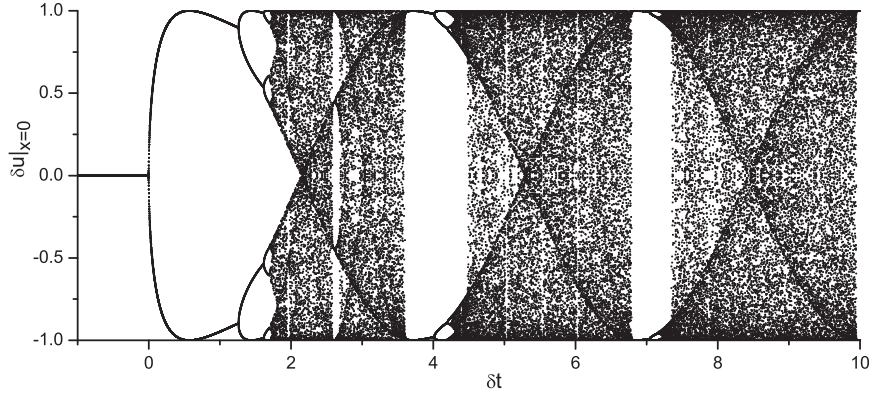


Fig. 5. The period-doubling bifurcation diagram shows dependence on the parameter δt of disturbance of the center of the “tyger”.

$$u + \delta u = \sin(x - (u + \delta u)(t_* + \delta t)). \quad (12)$$

The relation between the disturbance of the position of the “tyger”’s center ($x = 0$) and the time perturbation δt is obtained from Eq. (11) and Eq. (12)

$$\delta u = \sin(\delta u(t_* + \delta t)). \quad (13)$$

Eq. (13) similarly to Eq. (9) can also be reduced to a map with δt as a bifurcation parameter

$$g_1 : \delta u_{n+1} = \sin(\delta u_n(t_* + \delta t)). \quad (14)$$

The period-doubling bifurcation diagram of the map (14) is shown in Fig. 5. The equilibrium position of the disturbance remains to be zero as $\delta t \leq 0$ and splits into two branches beyond $\delta t = 0$ via a period-doubling bifurcation. After a series of bifurcations, the system enters a chaotic state at the instant of time $\delta t = 1.73$ which suggests a thermalized solution of the inviscid Burgers equation after a finite time.

4. Stability of nonlinear waves

In order to study the birth of early “tyger” depending on the truncated wavenumber, the equation for a perturbation to the untruncated solution has been obtained in [10]

$$\partial_t u' + P_{K_G} \partial_x \left(uu' + \frac{(u')^2}{2} \right) = P_{K_G} \partial_x \left(u^< u^> + \frac{(u^>)^2}{2} \right), \quad (15)$$

where

$$u' = P_{K_G}(v - u), \quad (16)$$

$$u^< = P_{K_G} u, u^> = (I - P_{K_G}) u. \quad (17)$$

Eq. (15) can be rewritten in terms of the new time as following:

$$\begin{aligned} \frac{d}{d\tau} u' &= Au' + f, u'(0) = 0, \\ A &= -P_{K_G} \partial_x (u_* \bullet), \\ f &= P_{K_G} \partial_x \left(u_*^< u_*^> + \frac{(u_*^>)^2}{2} \right). \end{aligned} \quad (18)$$

The right hand side of Eq. (15) or f in Eq. (18) is considered as an input to the system. The operator A , defined in Eq. (18), describes the interaction between a perturbation and the untruncated solution u_* frozen at t_* and varying in a new shifted time τ . The perturbed wave in this section is imposed on the truncated solution directly. By using the complex oscillator system, it is found that the perturbed wave is amplified just before occurrence of the pre-shock.

4.1. Perturbed wave equation

Derivation of the perturbed wave equation is similar to that for Eqs. (15) and (18), but the perturbed wave δv is not induced by truncation of the solution. Instead, it is exerted to the existing wave, v_1 , artificially. In other words, information about the truncated wavenumber is not significant. The truncated wavenumber is chosen to be the same as in the previous section, $K_G = 700$. The behavior of the perturbed wave is restricted in the time domain $-\tau < t < \tau$ when the existing wave, v_1 , forms assuming that v_1 is considered to be frozen in the time variable τ . In order to obtain the perturbed wave equation within $-\tau < t < \tau$, let us replace the solution v in Eq. (4) by $v_1 + \delta v$. Then the perturbed wave equation is

$$\frac{\partial \delta v}{\partial \tau} + P_{K_G} \left(\left[\frac{\partial v_1}{\partial x} + v_1 \frac{\partial}{\partial x} \right] \delta v \right) + P_{K_G} \left(\delta v \frac{\partial \delta v}{\partial x} \right) = 0. \quad (19)$$

The terms in the brackets represent interaction between the existed wave profile and the perturbed wave. The stability of the wave profile v_1 at t_1 is determined by behavior of the perturbed wave coupled with that profile near this moment. Therefore, it is reasonable to assume that the amplitude of the perturbed wave is much smaller than that of the existing nonlinear wave profile,

$$|\delta v| \ll |v_1(x, \tau)|. \quad (20)$$

Eq. (19) can be reduced in this case to a linear perturbed wave equation via a linearization near the wave profile by neglecting the nonlinear term

$$\begin{aligned} \frac{d}{d\tau} \delta v &= A \delta v, \\ A &= -P_{K_G} \left(\left(\frac{\partial v_1}{\partial x} + v_1 \frac{\partial}{\partial x} \right) \bullet \right). \end{aligned} \quad (21)$$

There is no beating input to the system as compared to Eq. (18). Moreover, the initial condition is unnecessary, because behavior of the perturbed wave is predicted through an eigenvalue problem for a complex oscillator system. In spite of neglecting the nonlinear term, the nonlinear feature is kept partially in the coupling with the nonlinear waves. Besides, the linear perturbed wave system is similar to the linear equation in [19] to study the generation of “tygers”.

4.2. Complex oscillator system

The tendency of motion of the perturbed wave is derived from the eigenvalue problem for a linear perturbed wave equation. It is equivalent to a transformation of the perturbed wave system into a complex oscillator system. Then the eigenvalue problem is studied for that system [20]. Considering the complex oscillator system with N oscillators, the k th oscillator is represented by $(x_k + iy_k)$. The motion in two orthogonal directions x_k and y_k are described by the following equations:

$$\frac{dx_k}{dt} = F_k(x_k, y_k, x_{j \neq k}, y_{j \neq k}), \quad (22a)$$

$$\frac{dy_k}{dt} = G_k(x_k, y_k, x_{j \neq k}, y_{j \neq k}), \quad (22b)$$

where $(k, j = 1, 2, \dots, N)$. Generally speaking, F_k and G_k depend on oscillators $\{x_k, y_k\}$. Then the k th oscillator interacts with the other $N - 1$ oscillators. Eq. (22b) describes a coupled nonlinear complex oscillator system.

Perturbations are imposed in every direction of motion of the oscillator $(x^1 + iy^1)$. For example, one gets for the k th oscillator

$$x_k(t) = x_k^1(t) + \delta x_k(t), \quad y_k(t) = y_k^1(t) + \delta y_k(t). \quad (23)$$

Replacing $x^1 + iy^1$ by $(x^1 + \delta x) + i(y^1 + \delta y)$, a linear perturbation equation is arrived. Let $\delta z = [\delta x_1, \delta y_1, \delta x_2, \delta y_2, \dots, \delta x_N, \delta y_N]^T$, then the linear perturbation equation is

$$\frac{d\delta z}{dt} = [H] \cdot \delta z, \quad (24)$$

where δz is a $2N \times 1$ matrix and $[H]$ is a $2N \times 2N$ matrix. The elements of $[H]$ are the following:

$$H_{2k-1,2j-1} = \partial F_k / \partial x_j, \quad (25a)$$

$$H_{2k-1,2j} = \partial F_k / \partial y_j, \quad (25b)$$

$$H_{2k,2j-1} = \partial G_k / \partial x_j, \quad (25c)$$

$$H_{2k,2j} = \partial G_k / \partial y_j. \quad (25d)$$

Eigenvalue function is derived from Eq. (24)

$$|H - \lambda I| = 0, \quad (26)$$

where I is $2N \times 2N$ unit matrix.

In order to specify the coupling between the nonlinear and perturbed waves, we expand the wave solution and the perturbed wave into the Fourier series

$$\nu_1(x) = \sum_{k=1}^{K_G} A_k \cos(kx + \theta_k), \quad (27)$$

$$\delta\nu(x, \tau) = \sum_{k=1}^{K_G} b_k(\tau) e^{ikx + \alpha(\tau)} + c.c. \quad (28)$$

The conjugated term in Eq. (28) implies that the perturbed wave travels in the opposite directions, x and $-x$. Substituting them to Eq. (21), we get equations for the mode amplitudes and phases $\{b_k, \alpha_k\}$ of the perturbed wave

$$\begin{aligned} \frac{db_k}{d\tau} &= +\frac{k}{2} \left\{ \sum_{i+j=k} A_i b_j \sin(\theta_i + \alpha_j - \alpha_k) + \sum_{i-j=k} A_i b_j \sin(\theta_i - \alpha_j - \alpha_k) + \sum_{-i+j=k} A_i b_j \sin(-\theta_i + \alpha_j - \alpha_k) \right\}, \\ \frac{d\alpha_k}{d\tau} &= -\frac{k}{2b_k} \left\{ \sum_{i+j=k} A_i b_j \cos(\theta_i + \alpha_j - \alpha_k) + \sum_{i-j=k} A_i b_j \cos(\theta_i - \alpha_j - \alpha_k) + \sum_{-i+j=k} A_i b_j \cos(-\theta_i + \alpha_j - \alpha_k) \right\}. \end{aligned} \quad (29)$$

The nonlinear and perturbed waves can also be represented by the complex oscillator systems $\{X_k + iY_k\}$ and $\{x_k + iy_k\}$, respectively, using the definitions

$$X_k = A_k \cos \theta_k, Y_k = A_k \sin \theta_k, \quad (30)$$

$$x_k = b_k \cos \alpha_k, y_k = b_k \sin \alpha_k. \quad (31)$$

Thus the expressions for F_k and G_k in Eq. (22b) can be obtained from Eq. (29)

$$\begin{aligned} F_k &= +\frac{k}{2} \left\{ \sum_{i+j=k} (Y_i x_j + X_i y_j) + \sum_{i-j=k} (Y_i x_j - X_i y_j) + \sum_{-i+j=k} (-Y_i x_j + X_i y_j) \right\}, \\ G_k &= -\frac{k}{2} \left\{ \sum_{i+j=k} (X_i x_j - Y_i y_j) + \sum_{i-j=k} (X_i x_j + Y_i y_j) + \sum_{-i+j=k} (-X_i x_j + Y_i y_j) \right\}. \end{aligned} \quad (32)$$

The elements $[H]$ of the eigenvalue function Eq. (26) are derived from Eqs. (25d) and (32). One gets for the elements with $m = n$

$$\begin{aligned} H_{2n-1,2m-1} &= +\frac{1}{2} n Y_{2n}, H_{2n-1,2m} = -\frac{1}{2} n X_{2n}, \\ H_{2n,2m-1} &= -\frac{1}{2} n X_{2n}, H_{2n,2m-1} = -\frac{1}{2} n X_{2n}, \end{aligned} \quad (33)$$

for the elements with $m > n$

$$\begin{aligned} H_{2n-1,2m-1} &= +\frac{1}{2} n (-Y_{m-n} + Y_{m+n}), H_{2n-1,2m} = -\frac{1}{2} n (-X_{m-n} + X_{m+n}), \\ H_{2n,2m-1} &= -\frac{1}{2} n (X_{m-n} + X_{m+n}), H_{2n,2m} = -\frac{1}{2} n (Y_{m-n} + Y_{m+n}), \end{aligned} \quad (34)$$

and for the elements with $m < n$

$$\begin{aligned} H_{2n-1,2m-1} &= +\frac{1}{2} n (Y_{n-m} + Y_{n+m}), H_{2n-1,2m} = +\frac{1}{2} n (X_{n-m} + X_{n+m}), \\ H_{2n,2m-1} &= -\frac{1}{2} n (X_{n-m} + X_{n+m}), H_{2n,2m} = +\frac{1}{2} n (Y_{n-m} - Y_{n+m}). \end{aligned} \quad (35)$$

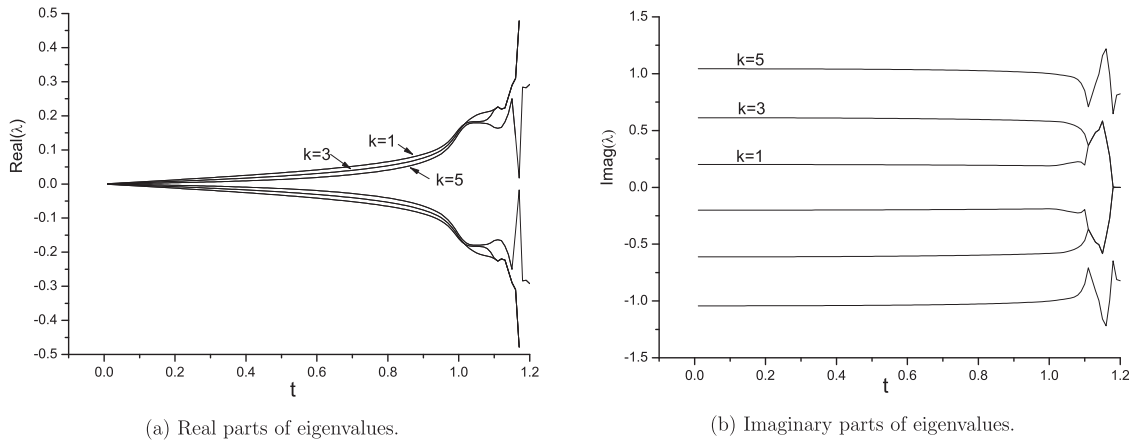


Fig. 6. Real and imaginary parts of eigenvalues of the perturbed oscillators of low order.

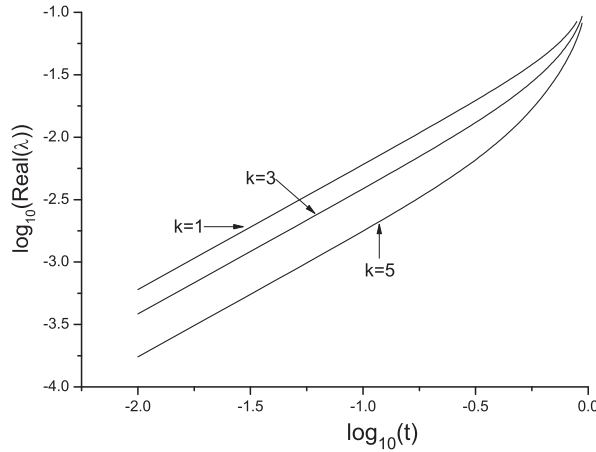


Fig. 7. Scale laws for the positive real parts of eigenvalues of the low order.

4.3. Evolution of eigenvalues of the perturbed wave

$2N$ eigenvalues of Eq. (26) are obtained after diagonalization of the matrix $[H]$. Their real parts are usually used for predicting whether a perturbed wave is amplified or suppressed. Imaginary parts usually represent frequency of the perturbed wave oscillator. The wave solution at every moment in the range $0 < t_1 < t_*$ determines uniquely one oscillator system $\{X_k, Y_k\}$ leading to K_G pairs of the conjugate complex eigenvalues $\{\lambda_k = \text{Real}(\lambda_k) \pm i\text{Imag}(\lambda_k)\}$ from Eq. (26). Therefore, $2K_G$ functions of real and imaginary parts of the eigenvalues could be established with respect to time during the interval $0 < t < t_*$. It is worth to note that the k th pair of the complex eigenvalues does not represent motion of the k th perturbed oscillator directly due to existence of the interaction of this oscillator with the other $K_G - 1$ oscillators.

As shown in Fig. 6, the perturbed oscillators are unstable in low order even far from the critical time $t_1 \ll t_*$. The real parts of the conjugated eigenvalues split from zero into two branches, a positive one and its opposite number, as early as $t_1 = 0$. The positive real part, as well as its negative conjugated one, implies that the perturbed oscillations are amplified in one direction and suppressed in the orthogonal one. The real parts grow faster before the critical time, especially, for the first order of the perturbed oscillator. They grow as shown in Fig. 7. Beyond t_* , they grow even faster, but some of them begin to oscillate. The imaginary parts begin to converge to zero near t_* after oscillations.

Motion of perturbed oscillators of the high order shows very different features from that of the low order. The real parts of them remain zero before t_* , which suggests a critical state. In other words, the motion of perturbed oscillators of the high order are neither amplified nor suppressed. Until the time approaches to t_* , the real parts split into a positive one and a negative one abruptly and diverge drastically. More importantly, the unstable modes of the perturbed oscillator of the higher order are exited later than that of the lower order, (Fig. 8). In summary, the perturbed waves in every order are unstable near t_* , when a shock occurs in the wave solution.

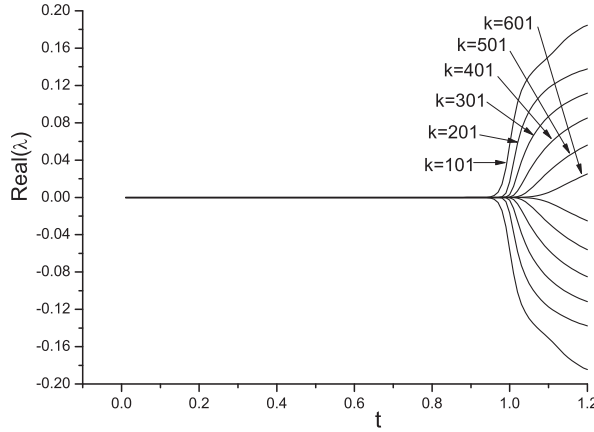


Fig. 8. Real parts of eigenvalues of the perturbed wave of the high order.

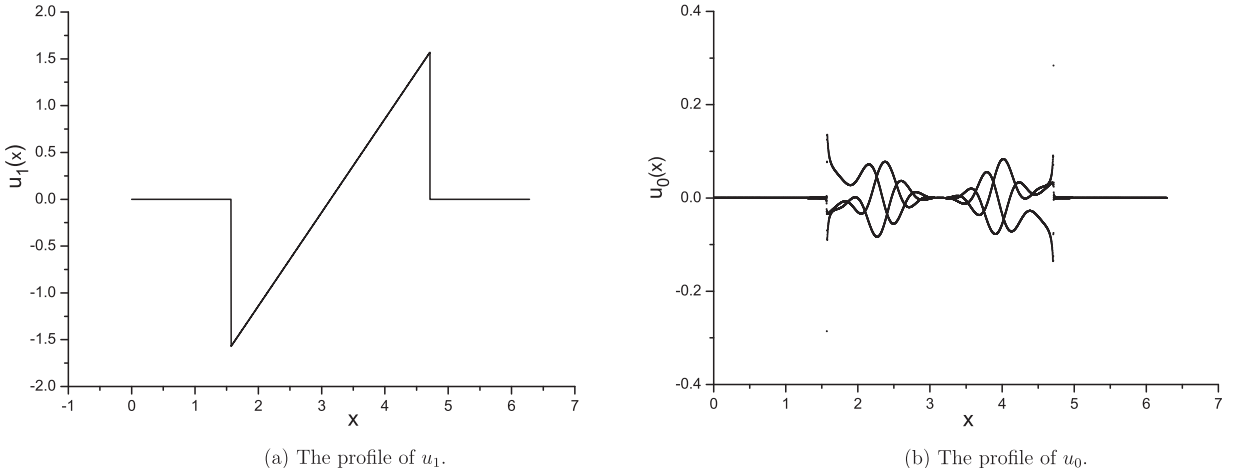


Fig. 9. The wave profile for u_1 (a) and initial profile for u_0 (b).

5. Transition from the “tyger” to thermalization

Stability analysis beyond t_* is no longer valid because the perturbed wave is not small enough, or Eq. (20) is no longer valid. The nonlinear term in Eq. (19) cannot be neglected. Thus, Eq. (19) is rewritten as Eq. (36)

$$\frac{\partial \delta v}{\partial \tau} + P_{K_G} \left(\left[\frac{\partial u_1}{\partial x} + u_1 \frac{\partial}{\partial x} \right] \delta v \right) + P_{K_G} \left(\delta v \frac{\partial \delta v}{\partial x} \right) = 0, \\ v(x, 0) = P_{K_G} u(x). \quad (36)$$

The wave profile u_1 , containing a shock, is frozen at t_* . Here u_1 is chosen artificially with a pair of shocks in symmetry. As a matter of fact, the nature of shocks is studied in [18,21–23]. Following their ideas, a shock in the wave profile u_1 is considered as a discontinuity or a strong velocity gradient in the wave solution. The wave pattern u_1 is described by a discontinuous function as

$$u_1(x) = \begin{cases} x & \pi/2 < x < 3\pi/2, \\ 0 & \text{others}, \end{cases} \quad (37)$$

which is shown in Fig. 9(a). The initial condition is obtained as a difference between the wave solution at a small time instant and the initial condition for u_1 in Eq. (4)

$$u_0(x) = u|_{t=0.001} - u_1, \quad (38)$$

which is illustrated in Fig. 9(b). It is obvious that small local structures have already formed immediately after beginning of simulation of Eq. (4).

The process of thermalization is illustrated in Fig. 10 which is depicted as a scattering diagram. The structures spread and occupy the entire domain quickly as shown in Fig. 10(a). But after formation of the structures, they become very stable.

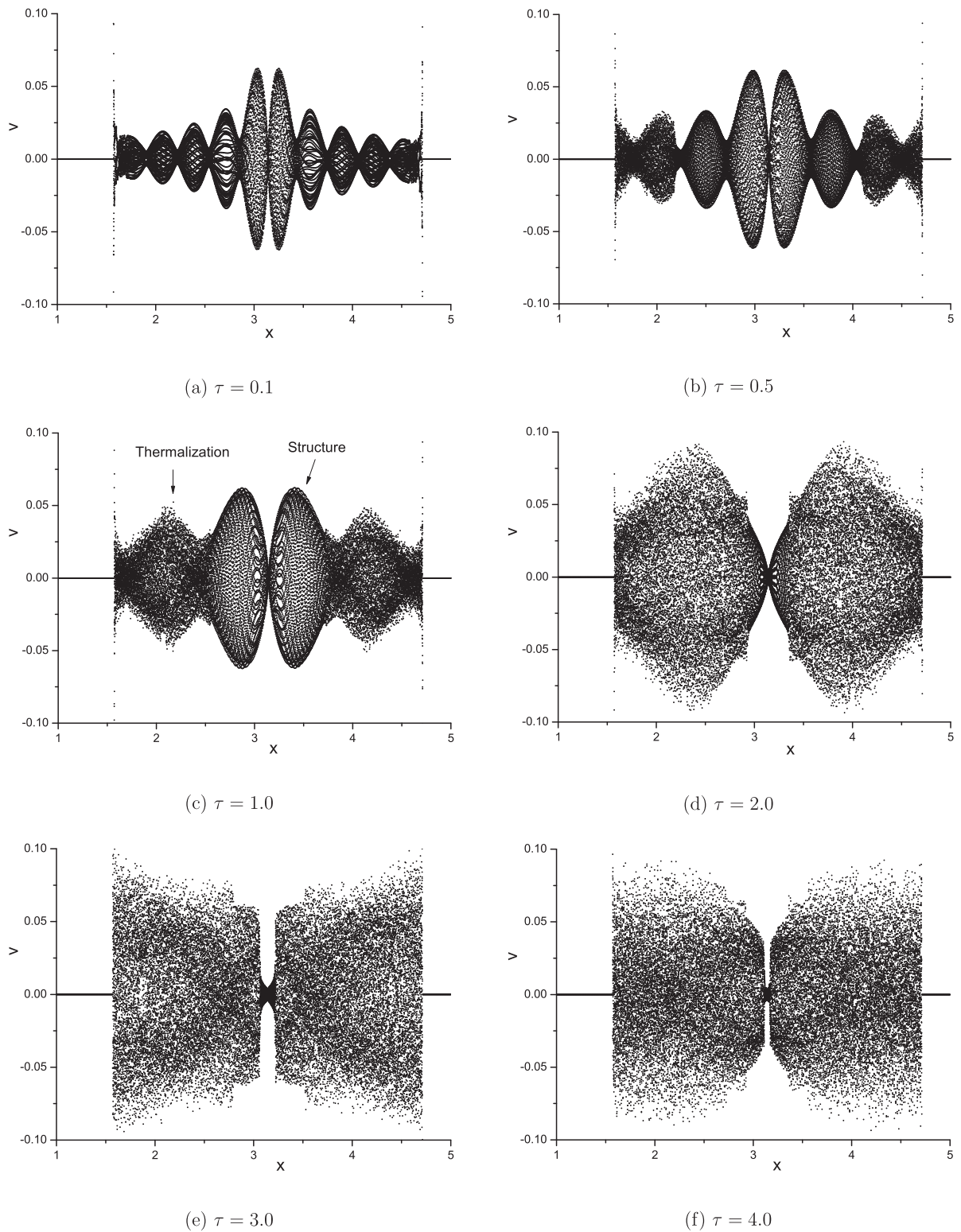


Fig. 10. Evolution from a “tyger” state to final thermalization.

More importantly, the thermalization begins from the both sides of the structures, and the range of thermalization expands to the center of the domain very slowly. Finally, the thermalized solution occupies the whole domain. It is worth to note that the structures can maintain their shapes before thermalization without symmetry breaking in this process.

6. Conclusions

The Galerkin-truncated solution of the inviscid Burgers equation diverges from the exact solution after occurrence of a pre-shock which is represented by the birth of “tygers”. The “tygers” may have very different shapes if the truncated projector P_{K_G} acts on nonlinear term in a different way. The period-doubling bifurcation is related to the birth of “the tygers” from a map constructed by the iterative method.

Loss of stability of the truncated solution can be understood due to behavior of the perturbed wave. It is found from analysis of the eigenvalue problem that low-order modes of the perturbed wave lose their stability even far from the critical time t_* . The high-order modes are amplified near the occurrence of a pre-shock at t_* . The perturbed waves are unstable in each mode of the perturbed oscillator near t_* .

Finally, the transition from a “tyger” to a thermalization is a long-term process. Small local structures, coupled with a frozen wave with a pair of shock waves in symmetry, grow in the whole domain gradually. At the very beginning of generation of local structures, the thermalization begins from the both sides of boundaries to the center of the coherent structures until the entire structure is thermalized.

Acknowledgments

The research is supported by the National Basic Research Program of China (973 Program, Grant No. 2012CB026002), the National Key Technology R&D Program of China (Grant No. 2013BAF01B02) and the [National Natural Science Foundation of China](#) (Grant No.[51305355](#)).

References

- [1] Frisch U. *Turbulence: the Legacy of an Kolmogorov*. Cambridge University Press; 1995.
- [2] Kolmogorov AN. The local structure of turbulence in incompressible viscous fluid for very large Reynolds numbers. In: *Dokl. Akad. Nauk SSSR*, vol. 30; 1941. p. 299–303.
- [3] Hopf E. The partial differential equation $ut + uux = \mu xx$. *Commun Pure Appl Math* 1950;3(3):201–30.
- [4] Lee T. On some statistical properties of hydrodynamical and magnetohydrodynamical fields. *Q Appl Math* 1952;10(1):69–74.
- [5] Kraichnan RH, Nagarajan S. Growth of turbulent magnetic fields. *Phys. Fluids (1958–1988)* 1967;10(4):859–70.
- [6] Kraichnan RH, Chen S. Is there a statistical mechanics of turbulence? *Phys. D* 1989;37(1):160–72.
- [7] Cichowlas C, Bonaïti P, Debbasch F, Brachet M. Effective dissipation and turbulence in spectrally truncated euler flows. *Phys. Rev Lett* 2005;95(26):264502.
- [8] Frisch U, Kurien S, Pandit R, Pauls W, Ray SS, Wirth A, et al. Hyperviscosity, galerkin truncation, and bottlenecks in turbulence. *Phys Rev Lett* 2008;101(14):144501.
- [9] Nazarenko S, Onorato M, Proment D. Bose-einstein condensation and berezinskii-kosterlitz-thouless transition in the two-dimensional nonlinear Schrödinger model. *Phys Rev A* 2014;90(1):013624.
- [10] Ray SS, Frisch U, Nazarenko S, Matsumoto T. Resonance phenomenon for the galerkin-truncated burgers and euler equations. *Phys Rev E* 2011;84(1):016301.
- [11] Venkataraman D, Ray SS. The onset of thermalisation in finite-dimensional equations of hydrodynamics: insights from the burgers equation[J]. arXiv:160807574, 2016.
- [12] Frisch U, Pomyalov A, Procaccia I, Ray SS. Turbulence in noninteger dimensions by fractal fourier decimation. *Phys Rev Lett* 2012;108(7):074501.
- [13] Ray SS. Thermalized solutions, statistical mechanics and turbulence: an overview of some recent results. *Pramana* 2015;84(3):395–407.
- [14] Peyret R. *Spectral Methods for Incompressible Viscous Flow*, vol. 148. Springer; 2002.
- [15] Hou TY, Li R. Computing nearly singular solutions using pseudo-spectral methods. *J Comput Phys* 2007;226(1):379–97.
- [16] Fournier J, Frisch U, de m6c. Th6or et Appl 1983;2:699–750.
- [17] Buzzicotti M, Biferale L, Frisch U, Ray SS. Intermittency in fractal fourier hydrodynamics: lessons from the burgers equation. *Phys Rev E* 2016;93(3):033109.
- [18] Zhang J-Z, Liu Y, Ren X-L, Duan S-M. Saddle-node bifurcations in burgers equation as shock wave occurrence. In: *Nonlinear Science and Complexity (NSC), 2012 IEEE 4th International Conference on*. IEEE; 2012. p. 195–200.
- [19] Banerjee D, Ray SS. Transition from dissipative to conservative dynamics in equations of hydrodynamics. *Phys Rev E* 2014;90(4):041001.
- [20] He K. Embedded moving saddle point and its relation to turbulence in fluids and plasmas. *Int J Modern Phys B* 2004;18(13):1805–43.
- [21] Wang Z, Zhang J, Ren J, Aslam MN. A geometric singular perturbation approach for planar stationary shock waves. *Phys D* 2015;310:19–36.
- [22] Ablowitz MJ, Baldwin DE. Dispersive shock wave interactions and asymptotics. *Phys Rev E* 2013;87(2):022906.
- [23] Ablowitz M, Baldwin D, Hoefer M. Soliton generation and multiple phases in dispersive shock and rarefaction wave interaction. *Phys Rev E* 2009;80(1):016603.